Universidad de Cádiz

Intelligent Control Algorithm for Power Balance Between Microgrids

Carrasco González, David; Sarrias Mena, Raúl; Horrillo Quintero, Pablo; Llorens Iborra, Francisco; Fernández Ramírez, Luis Miguel

Published in:
2023 IEEE 2nd Industrial Electronics Society Annual On-Line Conference, ONCON 2023

DOI (link to publication from Publisher):
10.1109/ONCON60463.2023.10431261

Publication date:
2024

Document Version:
Camera ready

Citation for published version (IEEE):
D. Carrasco-Gonzalez, R. Sarrias-Mena, P. Horrillo-Quintero, F. L. Iborra, and L. M. Fernandez-Ramirez, "Intelligent Control Algorithm for Power Balance Between Microgrids" 2023 IEEE 2nd Industrial Electronics Society Annual On-Line Conference, ONCON 2023, 2023, doi: 10.1109/ONCON60463.2023.10431261.

Intelligent Control Algorithm for Power Balance Between Microgrids

David Carrasco-González[1], Raúl Sarrias-Mena[2], Pablo Horrillo-Quintero[1], Francisco Llorens Iborra[1], and Luis M. Fernández-Ramírez[1]
[1] *SURET Research Group, Department of Electrical Engineering, University of Cadiz (UCA)*, ETSI Algeciras, Spain
[2] *SURET Reseach Group, Dept. of Engineering in Automation, Electronics and Computer Arch. and Networks, UCA*, ETSI Algeciras, Spain
david.carrasco@uca.es, raul.sarrias@uca.es, pablo.horrillo@uca.es, francisco.llorens@uca.es, luis.fernandez@uca.es

***Abstract*—Microgrid clusters are becoming increasingly popular owing to their many benefits and their ability to meet human needs in terms of energy flexibility, security, and integration of renewable sources. They are composed of interconnected microgrids with a variety of power generation sources, loads, and storage devices. Microgrid clusters can also combine DC and AC technologies, even within a single microgrid. In this work, a new energy management system is developed for a microgrid cluster consisting of two microgrids connected to the main grid. The proposed energy management system, acting as the centralized control layer in the microgrid cluster, is based on a fuzzy-logic algorithm. The microgrid cluster consists of an AC microgrid integrating a photovoltaic generator, a battery bank and AC loads; and a DC microgrid composed of a wind turbine, electrolyzer, ultracapacitor, fuel cell and DC loads. The microgrid cluster is tested under different working conditions, such as variable wind speed and solar irradiance, and connection and disconnection of the loads. Finally, the energy management system implemented in the microgrid cluster exhibits a correct behaviour under different conditions, according to the results obtained.**

Keywords—Energy management system, fuzzy-logic, microgrid cluster.

I. Introduction

The utilization of renewable energy sources in electricity generation is becoming increasingly important in the fight against climate change. The desired reduction in greenhouse gas emissions, which are the main cause of climate change [1], requires substituting fossil fuels with cleaner sources. In addition, the exponential growth of power demand in industries and cities, coupled with the need for more resilient and sustainable energy systems, generate the need to convert conventional grids into small-scale grids that can operate autonomously, denoted as microgrids (MGs) [2]. These are attractive solutions owing to their improved power quality and reliability, reduced carbon emissions, higher energy efficiency, and economic benefits [3].

An MG is constituted by a collection of renewable energy sources, energy storage systems (ESSs), and distributed loads, with specified electrical boundaries, and functions as a cohesive and controllable system [4], [5]. AC MGs have been investigated due to their compatibility with conventional grids; however, DC MGs have gained increasing attention in recent years [6]. Thus, MGs can be operated by employing DC, AC, or a combination of AC/DC technologies, providing greater flexibility and adaptability [7].

This work was partially supported by Ministerio de Ciencia e Innovación, Agencia Estatal de Investigación, FEDER, UE (Grant PID2021-123633OB-C32 supported by MCIN/AEI/10.13039/501100011033/ FEDER, UE).

A MG can operate autonomously and isolated; this situation is frequent in remote areas with limited or no access to a main grid. The characteristics of a stand-alone MG were analysed in [8]. Despite this, MGs are usually connected to a main grid through the point of common coupling (PCC). This fact allows them to operate in two different modes: a) grid-connected mode, where the main grid can supply power during deficits in the MG or can absorb power during excesses in the MG [9]; and b) islanded mode, where the electricity produced in the MG can only be held by the ESSs or consumed by the loads [10].

In this situation, multiple adjacent MGs can be interconnected and operated in a coordinated manner to form a microgrid cluster (MGC). This association provides several benefits, including: 1) it facilitates the integration of different power systems in the MGs; 2) it facilitates the decentralization of the power system; 3) it allows to increase and consolidate the local electricity generation and consumption; and 4) it improves reliability, resiliency, sustainability and efficiency [11].

To reach the desired objectives of the MGs, energy management systems (EMSs) are employed in different ways to obtain the power references of the power sources within an MG [12], [13]. Recently, there has been growing interest in the employment of new algorithms in power systems, such as model predictive control, genetic algorithm, and fuzzy-logic. Fuzzy-logic was employed in [14] in the secondary control to adjust the frequency and voltage in islanded MGs. An improved droop control method, based on fuzzy control, was adopted in a DC MG to improve the robustness of the system [15]. A fuzzy-logic EMS was presented in [16] for a residential grid-connected MG. However, this EMS does not consider the transient states of the system. Additionally, all these papers do not apply a fuzzy-logic control algorithm to manage the MGs in a MGC.

In this sense, this paper presents a new centralized EMS control for a MGC composed of a DC MG and an AC MG connected to a main grid. This EMS involves the use of fuzzy-logic algorithm permitting the cooperative control in the MGC, which allows the regulation of the MGs that constituted the MGC in different operating conditions.

The remainder of this paper covers the following aspects. Section II explains the configuration of the MGC and its controls. The EMS, based on fuzzy-logic controller, employed in the system is described in Section III. In Section IV, the results are presented and discussed. Finally, the conclusions of this study are presented in Section V.

II. Configuration and Control of the Microgrids

The MGC structure is presented in Fig. 1. It consists of a DC MG, an AC MG, and a connection to the main grid. A general description of the control concept applied on the components of each MG is that they are controlled individually and independently to follow a certain reference. Above these independent controllers, an EMS, based on a fuzzy-logic algorithm, coordinates the operation of all the components within the MGC, including generators, ESSs, loads and the main grid. In this sense, subsequent subsections present a detailed description of each MG and their controllers.

A. AC Microgrid

The AC MG consists of a Li-ion battery ESS (BESS), a photovoltaic (PV) generator, and local AC loads. These components of the MG are connected to a three-phase PCC. The other MG and the main grid are both connected to this PCC to complete the configuration of the MGC.

A PV power plant is considered in the AC MG. The PV panels are represented by a controlled current source plus one parallel diode model [17]. This model also includes series and parallel resistances. The PV panels are connected to a DC boost converter, which increases the voltage and implements a MPPT strategy for the PV generator. The classic Perturb and Observe (P&O) algorithm is employed to define the duty cycle of the boost converter to maximize the PV generation. A voltage source inverter (VSI) is then utilized to ensure the compatibility of the DC power with the AC grid, being the AC voltage and frequency imposed by the main grid. This inverter is controlled to regulate the DC voltage at the output of the boost converter to a constant value. A cascaded control loop based on PI regulators is implemented for this purpose [18].

A Li-ion BESS is used in the AC microgrid. The BESS is modelled using a controlled voltage source with a resistance connected in series. This BESS is connected to the PCC of the AC MG through a VSI, which is controlled to adjust the active and reactive power exchanged among this element and the rest of the system employing a cascaded control loop.

The AC microgrid is completed with the local loads. Two three-phase constant R-L loads, in a star arrangement, are considered. These loads are connected and disconnected from the AC microgrid at different time intervals to vary the power demand within the MGC and observe the response of the EMS and MG controllers.

B. DC Microgrid

The DC microgrid studied in this paper consists of a wind turbine (WT), ultracapacitor (UC), two loads and a hydrogen system, composed of an electrolyzer (EZ) and a fuel cell (FC), connected to a common DC bus, as shown in Fig. 1.

A synchronous generator modelled as a sixth-order system is considered for the WT [19]. After that, a combination of an uncontrolled bridge rectifier and a DC boost converter are employed to connect the generator to the DC bus. The rectifier allows transforming the AC power generated by the generator into DC power, and the boost converter regulates the speed of the WT to achieve the optimal operation under variable wind speed.

Regarding the ESSs, a bidirectional half-bridge converter implemented with IGBTs is used for connecting the UC. This structure allows charging and discharging the UC, exchanging energy with the DC bus in both directions. Because only energy consumption from the DC bus is feasible for the EZ, a buck converter is employed for this device. Similarly, a boost converter is used for the FC, because it can only supply energy to the common DC bus. The UC is modelled employing an ideal capacitor with a series resistor, the FC is represented using a controlled voltage source plus one diode model, and the EZ is modelled through a voltage source with a series resistor [19]–[22].

The DC loads are directly coupled to the DC bus of this MG. A circuit breaker is used to connect and disconnect these loads. These components do not require any power control capabilities.

Finally, a VSI connects the DC bus of this MG to the three-phase AC bus considered as the PCC of this MGC. This converter is responsible for maintaining a constant DC bus voltage under active power fluctuations among the elements of the MG derived from the variable wind speed and load changes, and for converting the DC power to the AC power of the grid.

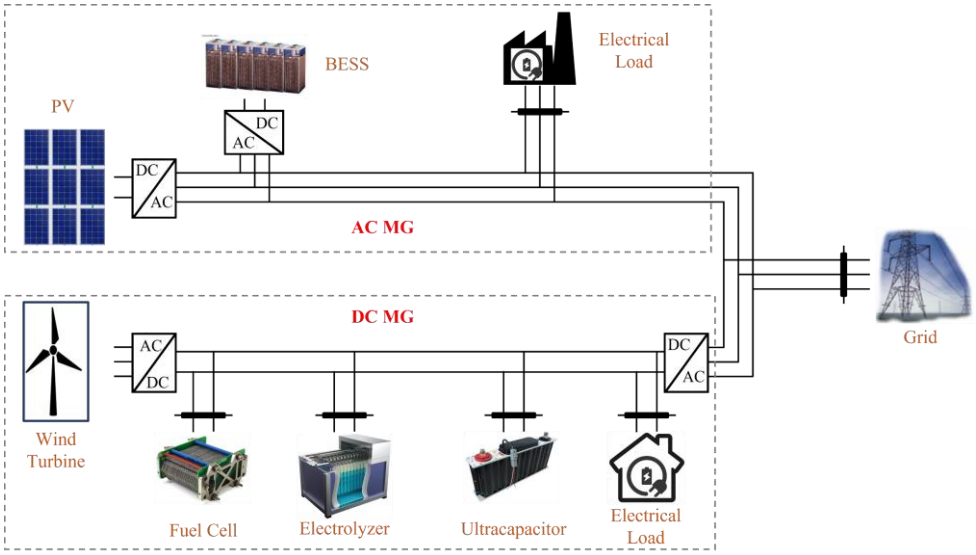

Fig. 1. MGC structure.

C. Main Grid

A stiff three-phase AC grid is considered as the main grid in the MGC. This element is modelled as an ideal three-phase AC voltage source with constant frequency and voltage. The main grid is connected to the PCC together with the AC and DC MGs. In this work, the MGC always operates in the grid-connected mode, and islanded operation is not considered.

Because the voltage and frequency at this point are maintained by the main grid, no control actions are required at this point, and the active and reactive power exchanges with the main grid are self-regulated to ensure the power balance and avoid voltage and frequency deviations.

D. MG Control

In this subsection, the MG controls implemented in the MGC are presented. For the PV generator, an MPPT strategy based on the P&O algorithm is employed to optimize the power generation from the solar radiation, which varies along the simulations performed. The wind speed is also a variable parameter. Hence, the speed of the WT is controlled to follow the optimal power curve under these circumstances.

The active power exchange of the ESSs is controlled to track the references provided by the EMS, employing PI regulators. In this sense, the BESS, UC, EZ and FC are required to follow the active power reference set by the EMS. For the UC and the BESS, positive and negative active power references are feasible, which imply discharging and charging these devices respectively. Contrarily, only negative power references can be provided to the EZ control loop, and positive values to the FC controller.

Finally, time-controlled circuit breakers are used to connect and disconnect AC and DC loads to each MG. These loads do not demand any specific control strategy, as they are considered in the EMS.

III. Fuzzy-Logic Energy Management System

The EMS proposed in this work is based on a fuzzy-logic algorithm. This EMS is responsible for defining the active power references for all the ESSs participating in the MGC. In terms of power balance, all MGs participating in the cluster are managed as a single unit, with all the power sources contributing to the same generation pool, all the loads demanding from a single consumption pool, and all the ESSs available to cover the gap between both profiles.

This fuzzy-logic EMS is designed for cooperative operation of the MGC, adopting a centralized control approach. It offers several advantages over decentralized control, including lower operation costs, simpler maintenance, enhanced efficiency and simple control architecture.

Therefore, the first step in the EMS is to calculate the active power mismatch between generation and demand, caused by the fluctuating operation of the renewable sources and the variable load profile. This difference must be covered by the ESSs, and their active power references are defined accordingly. Nevertheless, their contribution is sometimes compromised by their state-of-charge (SOC). For instance, BESSs are often required to remain within a safe operation SOC margin. Exceeding the minimum or maximum SOC limits may harm these devices. For such reason, the SOC of the BESSs is used as an input in the EMS proposed herein. Therefore, the power mismatch (calculated as the difference between the instantaneous active power generation of all MGs and the total instantaneous demand) and the SOC of the BESS are the two inputs of the fuzzy logic controller used in the EMS. The outputs of this controller are the active power references for the BESS, the EZ and the FC. The rules of the fuzzy logic controller are defined to satisfy the power demand taking into consideration the inherent characteristics of each ESS. In this sense, the first option is to use the BESS to cover the power mismatch because of its faster response compared to the hydrogen system. Nevertheless, this can only happen under certain circumstances. For instance, if the SOC of the BESS is near the minimum boundary, the discharge of the BESS will be limited or even restricted. In such case, the FC is responsible for providing the active power that cannot be extracted from the BESS. An analogous situation happens when the SOC of the BESS is near its maximum values and the EZ starts absorbing energy to produce hydrogen. In general terms, the hydrogen system acts as a backup storage for the BESS. The last stage of the EMS is the definition of the active power reference for the UC, which is calculated to compensate the deviations of the BESS, the EZ and the FC from their power references. Subsequently, the UC is expected to operate during short periods (i.e., the transitory state when the power reference of other ESS changes) and with a quick response, which matches the characteristics of this technology adequately.

In the fuzzy-logic controller designed, the power mismatch ($P_{mismatch}$) input contains five membership functions (MFs), corresponding to 'Negative High' (power consumption much larger than generation), 'Negative Low, 'Zero', 'Positive Low' and 'Positive High' (power generation much larger than consumption). The MFs are shown in Fig. 2.

The SOC_{BESS} input presents three MFs, namely 'Low', 'Mid' and 'High'. This parameter can vary from 0 to 100%, and the MFs are shown in Fig. 3.

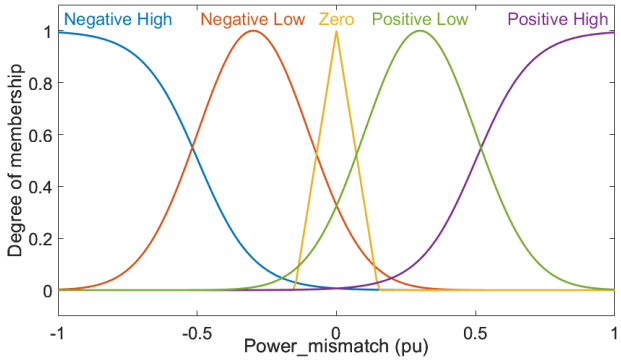

Fig. 2. Membership functions of $P_{mismatch}$.

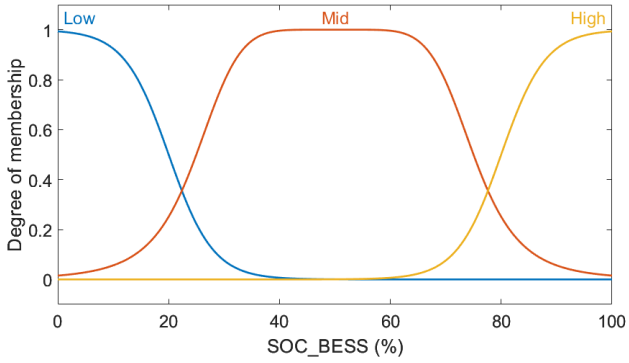

Fig. 3. Membership functions of SOC_{BESS}.

Three MFs are also used for $P_{BESS_{ref}}$, defined as 'Store', 'Standby' and 'Release'. Charging and discharging the BESS is accomplished with the 'Store' and 'Release' MFs respectively, whereas 'Standby' maintains the BESS output close to zero.

Since the power in the EZ ($P_{EZ_{ref}}$) and the FC ($P_{FC_{ref}}$) can only flow in one direction, only two MFs are defined for these devices. Both have a 'Standby' MF, which is defined to maintain a minimum non-zero power consumption and generation level in the EZ and the FC respectively, when they are not required to participate significantly. Additionally, the EZ has a 'Store' MF that allows hydrogen generation in the EZ; whereas the FC has a 'Release' MF to provide active power to the MGC consuming hydrogen. The MFs of the three outputs are shown in Figs. 4-6.

The fuzzy rules are defined to manage the participation of each ESS according to the instantaneous power mismatch and the SOC of the BESS. As an example, three possible situations are described below.

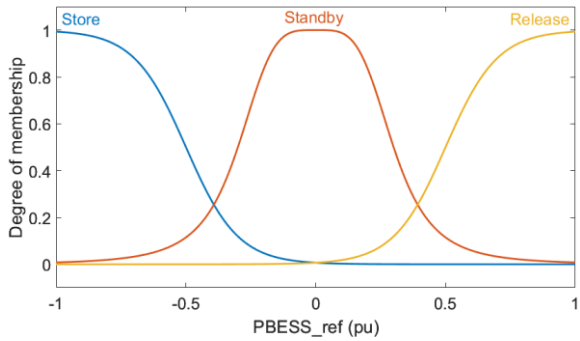

Fig. 4. Membership functions of $P_{BESS_{ref}}$.

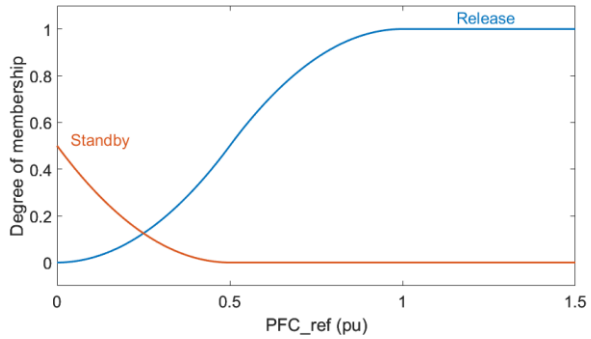

Fig. 5. Membership functions of $P_{FC_{ref}}$.

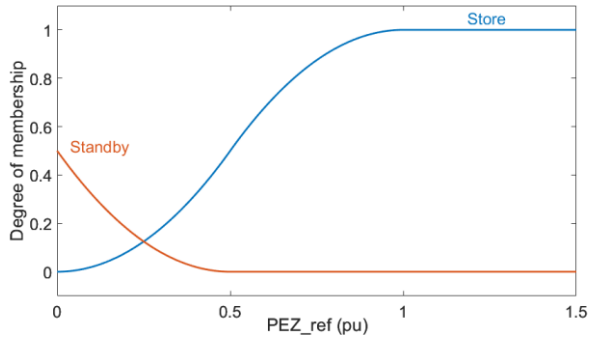

Fig. 6. Membership functions (MFs) of the $P_{EZ_{ref}}$.

If the power consumption largely exceeds generation ($P_{mismatch}$ is 'Negative High'), and the SOC of the BESS is 'Low', then the EZ is on 'Standby' absorbing the minimum operational power, the BESS will remain on 'Standby' to maintain its SOC and not to provide any energy, and the FC will 'Release' power to compensate the power mismatch between generation and demand and to protect the BESS against over-discharge.

The opposite situation occurs when $P_{mismatch}$ is 'Positive High' and SOC_{BESS} is 'High', using the EZ to store the excess power generation. The FC and the BESS remain in 'Standby' as no additional active power is necessary.

In an intermediate situation, $P_{mismatch}$ can vary from 'Positive Low' to 'Negative Low' with SOC_{BESS} in the 'Mid' range. In that scenario, the hydrogen system remains in 'Standby', and the BESS can 'Release' or 'Store' to compensate power deviations either absorbing or providing small power levels.

The outputs of the EMS are completed with the definition of the UC power reference, which covers the deviations of the active power absorbed/provided by each ESS and their references, as indicated previously.

IV. Results and Discussion

In this section, the MGC is tested in a 10 s simulation in Simulink to evaluate the performance, under different conditions, of the proposed control strategy and the EMS implemented in the MGC.

For the simulation presented, variable solar radiation and wind speed have been considered, that generate fluctuations in the PV and WT generation. Furthermore, the DC and AC loads are disconnected and connected from their corresponding buses at different time intervals. Finally, the SOC of the BESS is set to 50% at the beginning of the test, being in the middle of the minimum and maximum ranges.

Fig. 7 shows the active power exchange of all the ESSs in the MGC and their respective references. As seen in this figure, all the ESSs follow their respective active power reference adequately. This illustrates the satisfactory behaviour of the MG controllers.

When the renewable generation is higher than the load demand, the EMS defines that the ESSs store the surplus energy, and when the situation is the opposite, the EMS defines that the ESSs release energy to the MGC. The first situation occurs during two periods, from 1 to 1.5 s and from 3.75 to 5.25 s, approximately, whereas the second situation occurs during the rest of the simulation.

Since the SOC of the BESS is around 50%, this device is in the 'Mid' MF. Therefore, this device is set as the 'Store', 'Standby' or 'Release' MF depending on the power mismatch. Furthermore, the EZ and the FC support the BESS to reduce its SOC variation.

Finally, the UC contributes during the transitory deviations with large power peaks, and its active power tends to zero when the other ESSs approach their steady state.

Fig. 8 presents the electricity demand, the renewable energy generation, and the active power exchange with the main grid (P_{PCC}). The WT and PV generations vary when the solar irradiance and wind speed change. Additionally, the changes on the DC and AC loads power along the simulation

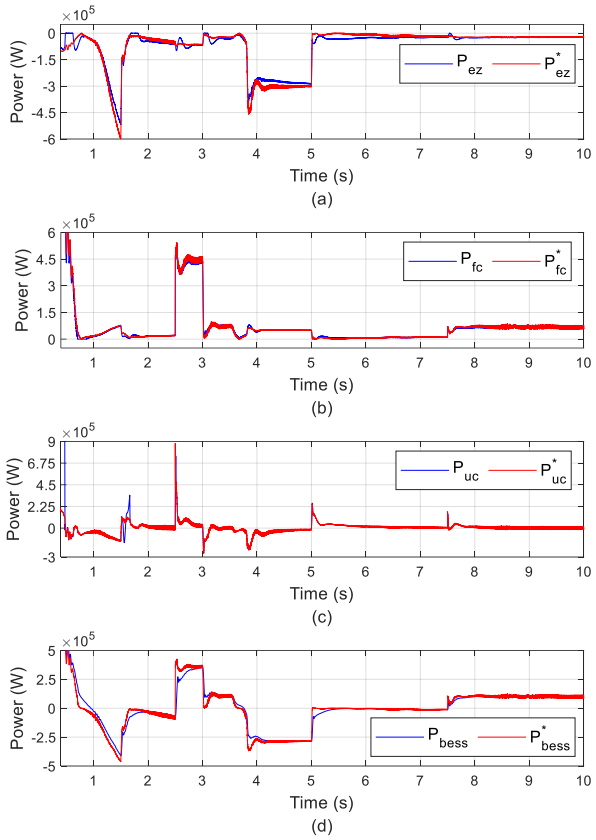

Fig. 7. Active power exchange of all the ESSs in the MGC: (a) EZ, (b) FC, (c) UC and (d) BESS.

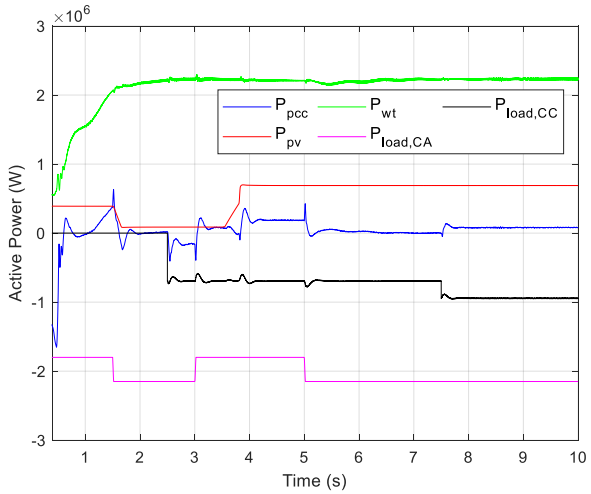

Fig. 8. Renewable power generation, load demand and active power exchange with the main grid (P_{PCC}).

are produced by the connection and disconnection of constant loads to each MG.

The DC load profile has slight fluctuations (Fig. 8). The DC and AC loads are introduced as constant current loads in the MGC, but fluctuations on the DC loads appear because of the flicker in the voltage of the DC bus. This effect is not visible on the AC load profile because the AC bus voltage is maintained constant by the main grid.

Finally, the main grid participates in the MGC when there is a modification in the solar irradiance, WT or the loads. It

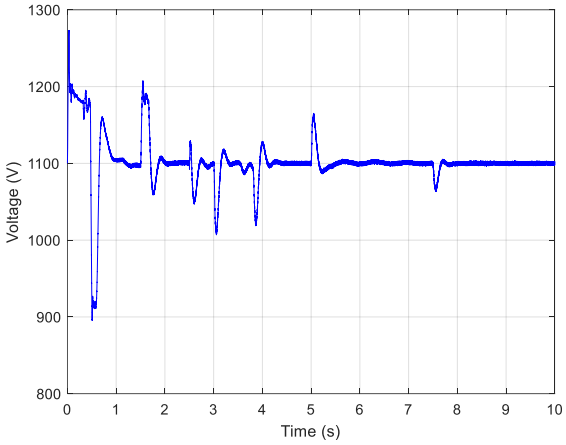

Fig. 9. DC bus voltage.

provides or absorbs the power imbalance that cannot be supported by the ESSs. When the active power among the generation and demand is balanced, its value tends to zero. Hence, this fuzzy-logic EMS allows to minimize the power exchange with the main grid.

The DC bus voltage throughout the simulation is illustrated in Fig. 9. This parameter is correctly regulated around its reference value, which is set to 1100 V. This adequate control is crucial because it allows a stable operation of all the components in the DC MG. As expected, modifications on the EZ, FC and UC operation, WT generation and DC load connection and disconnection, generate fluctuations on this voltage. However, this parameter is adequately regulated by the DC voltage control loop implemented on the VSI of the DC MG.

V. Conclusion

This work presented a new fuzzy-logic EMS for the dynamic control of a MGC composed of a hybrid DC-AC MGs and a main grid. The AC MG consists of a PV generator, a BESS bank and AC loads. On the other side, the DC MG consists of a WT, a UC, a hydrogen system (EZ plus FC) and DC loads. Both MGs were connected to a three-phase AC grid. The proposed control strategy was tested in a 10 s simulation in MATLAB/Simulink under several operating conditions, such as a variable wind speed and solar irradiance. Additionally, the electric loads were connected and disconnected from the system for various periods of time. The results presented in this paper showed an adequate performance of the MG controllers of the main elements of the MGC, and a successful coordination and power balance among the devices owing to the fuzzy-logic-based EMS implemented in the MGC. In addition, the power exchange with the main grid is minimized with this fuzzy-logic EMS.

References

[1] B. Atilgan and A. Azapagic, “Life cycle environmental impacts of electricity from fossil fuels in Turkey,” *J Clean Prod*, vol. 106, pp. 555–564, 2014, doi: 10.1016/j.jclepro.2014.07.046.

[2] I. Renewable Energy Agency, “Global Energy Transformation: A Roadmap to 2050,” 2018, Accessed: Mar. 03, 2023. [Online]. Available: www.irena.org

[3] D. E. Olivares *et al.*, “Trends in Microgrid Control,” *IEEE Trans Smart Grid*, vol. 5, no. 4, pp. 1905–1919, 2014, doi: 10.1109/TSG.2013.2295514.

[4] M. Shahbazitabar, H. Abdi, H. Nourianfar, A. Anvari-Moghaddam, B. Mohammadi-Ivatloo, and N. Hatziargyriou, “An Introduction to

Microgrids, Concepts, Definition, and Classifications," *Power Systems*, pp. 3–16, 2021, doi: 10.1007/978-3-030-59750-4_1.

[5] A. Vasilakis, I. Zafeiratou, D. T. Lagos, and N. D. Hatziargyriou, "The Evolution of Research in Microgrids Control," *IEEE Open Access Journal of Power and Energy*, vol. 7, pp. 331–343, 2020, doi: 10.1109/OAJPE.2020.3030348.

[6] L. de Oliveira-Assis *et al.*, "Optimal energy management system using biogeography based optimization for grid-connected MVDC microgrid with photovoltaic, hydrogen system, electric vehicles and Z-source converters," *Energy Convers Manag*, vol. 248, pp. 196–8904, 2021, doi: 10.1016/j.enconman.2021.114808.

[7] M. Najafzadeh, R. Ahmadiahangar, O. Husev, I. Roasto, T. Jalakas, and A. Blinov, "Recent Contributions, Future Prospects and Limitations of Interlinking Converter Control in Hybrid AC/DC Microgrids," *IEEE Access*, vol. 9, pp. 7960–7984, 2021, doi: 10.1109/ACCESS.2020.3049023.

[8] C. Zhang, X. Yang, and J. Wang, "Survey on Isolated Microgrid Prognostics and Health Management," *2022 2nd International Conference on Electrical Engineering and Control Science (IC2ECS)*, 2022, doi: 10.1109/IC2ECS57645.2022.10087926.

[9] Y. Guan, J. C. Vasquez, and J. M. Guerrero, "Hierarchical Controlled Grid-Connected Microgrid based on a Novel Autonomous Current Sharing Controller," *2015 IEEE Energy Conversion Congress and Exposition (ECCE)*, 2015, doi: 10.1109/ECCE.2015.7309988.

[10] D. Ioris, A. B. De Almeida, and P. T. De Godoy, "A microgrid islanding performance study considering time delay in island detection," *2020 IEEE PES Transmission and Distribution Conference and Exhibition - Latin America, T and D LA 2020*, Sep. 2020, doi: 10.1109/TDLA47668.2020.9326168.

[11] B. Chen, J. Wang, X. Lu, C. Chen, and S. Zhao, "Networked Microgrids for Grid Resilience, Robustness, and Efficiency: A Review," *IEEE Transactions on Smart Grid*, vol. 12, no. 1. Institute of Electrical and Electronics Engineers Inc., pp. 18–32, Jan. 01, 2021. doi: 10.1109/TSG.2020.3010570.

[12] Y. Zhou *et al.*, "Online energy management optimization of hybrid energy storage microgrid with reversible solid oxide cell: A model-based study," *J Clean Prod*, vol. 423, p. 138663, Oct. 2023, doi: 10.1016/J.JCLEPRO.2023.138663.

[13] Y. Guan, B. Wei, J. M. Guerrero, J. C. Vasquez, and Y. Gui, "An overview of the operation architectures and energy management system for multiple microgrid clusters," *iEnergy*, vol. 1, no. 3, pp. 306–314, Nov. 2022, doi: 10.23919/ien.2022.0035.

[14] N. B. De Nadai, A. C. Z. De Souza, J. G. C. Costa, C. A. M. Pinheiro, and F. M. Portelinha, "A secondary control based on fuzzy logic to frequency and voltage adjustments in islanded microgrids scenarios," *2017 IEEE Manchester PowerTech, Powertech 2017*, Jul. 2017, doi: 10.1109/PTC.2017.7981212.

[15] H. Liang, J. Ding, J. Bian, and Z. Liu, "Research on Fuzzy Droop Control of DC Microgrid Based on Consensus Algorithm," *4th International Conference on Smart Grid and Smart Cities, ICSGSC 2020*, pp. 76–82, Aug. 2020, doi: 10.1109/ICSGSC50906.2020.9248548.

[16] D. Arcos-Aviles, J. Pascual, L. Marroyo, P. Sanchis, F. Guinjoan, and M. P. Marietta, "Optimal Fuzzy Logic EMS design for residential grid-connected microgrid with hybrid renewable generation and storage," *IEEE International Symposium on Industrial Electronics*, vol. 2015-September, pp. 742–747, Sep. 2015, doi: 10.1109/ISIE.2015.7281561.

[17] M. A. Hasan and S. K. Parida, "An overview of solar photovoltaic panel modeling based on analytical and experimental viewpoint," *Renewable and Sustainable Energy Reviews*, vol. 60, pp. 75–83, Jul. 2016, doi: 10.1016/J.RSER.2016.01.087.

[18] A. Yazdani and I. Reza, *Voltage source converter in power system*. 2010. Accessed: Jul. 28, 2023. [Online]. Available: https://www.wiley.com/en-ca/Voltage+Sourced+Converters+in+Power+Systems+%3A+Modeling%2C+Control%2C+and+Applications-p-9780470521564

[19] R. Sarrias-Mena, L. M. Fernández-Ramírez, C. A. García-Vázquez, and F. Jurado, "Electrolyzer models for hydrogen production from wind energy systems," *Int J Hydrogen Energy*, vol. 40, no. 7, pp. 2927–2938, Feb. 2015, doi: 10.1016/J.IJHYDENE.2014.12.125.

[20] M. M. Rashid, M. N. Morshedul Haque, T. Akhtar, and M. S. Miah, "Simulink Model of Controlling Fuel Cell Powered Direct Current Motor with Comparative Performance Analysis," *Proceedings of the 4th International Conference on Communication and Electronics Systems, ICCES 2019*, pp. 1631–1637, Jul. 2019, doi: 10.1109/ICCES45898.2019.9002577.

[21] M. Albarghot and L. Rolland, "MATLAB/Simulink Modelling and Experimental Results of a PEM Electrolyzer Powered by a Solar Panel," *2016 IEEE Electrical Power and Energy Conference (EPEC)*, Dec. 2016.

[22] R. Jun, W. Kai, and L. Liwei, "Characteristics Analysis of Ultracapacitor-Battery Hybrid Energy Storage System," *2017 Chinese Automation Congress (CAC)*, 2018.